Short communication

Advanced nickel metal catalyst for water–gas shift reaction

Kyung-Ran Hwang, Chun-Boo Lee, Jong-Soo Park *

Korea Institute of Energy Research, 71-2 Jang-dong Yuseong-gu, Daejeon 305-343, Republic of Korea

ABSTRACT

A comparative study has been performed to investigate the effectiveness of a Ni metal catalyst before and after impregnation with potassium for the water–gas shift (WGS) reaction. The potassium-modified Ni metal is both more active and more selective for the WGS reaction than the unmodified Ni catalyst. Furthermore, there is no carbon deposition on the modified Ni catalyst. The amount of H_2 produced and the CO conversion via WGS over the potassium-modified Ni catalyst are higher than those for the commercial high-temperature shift (HTS) catalyst under severe experimental conditions (gas-hourly space velocity = $80\,000\,h^{-1}$, CO 60% and H_2 40%). The suppression of methanation over the modified Ni metal is attributed to the action of the incorporated potassium in increasing the density of the active hydroxyl group that takes part in the WGS reaction to form the intermediate.

© 2010 Elsevier B.V. All rights reserved.

1. Introduction

In recent years, the water–gas shift (WGS) reaction $(CO + H_2O \rightarrow CO_2 + H_2, \quad \Delta H = -41.1\,kJ\,mol^{-1})$ has been widely investigated in fuel cell technology. In a fuel processor, the two-stage WGS reactor occupies a large volume, i.e., ca. 70 vol.% of the whole system [1]. This presents a problem for mobile and automotive fuel processors. For miniaturization of portable fuel processor systems, advanced medium-temperature shift (MTS) catalysts applicable to a single-stage WGS reaction, mainly platinum-group metals on reducible oxide supports, have been investigated. As most MTS catalysts are ceramic-based catalysts with low thermal conductivity, however, the heat of the WGS reaction cannot be released rapidly to the reactor wall from the catalyst surface and this leads to the generation of hot spots and difficulties in enabling efficient operation close to the thermodynamic equilibrium. Thus, the authors have been investigating a catalytic active filter consisting of Pt/CeO_2 catalyst and metal as the heat-transfer media to improve the catalytic performance of the exothermic WGS reaction [2]. The results have indicated that tight contact of a metal with high thermal conductivity to the MTS catalyst enables the performance of the WGS reaction to be enhanced remarkably.

Ni-based catalysts have been recognized as an alternative catalyst [3,4]. For exothermic reactions because of their high heat-conductivity that facilitates control of the heat of reaction and allows a higher catalytic conversion to be maintained with the isothermal conditions in the catalyst bed. In addition, the Ni metal powder can be fabricated in various shapes by mould-pressing and tape-casting methods [4,5], which allows the volume of the processor system to be reduced. Unfortunately, the Ni-based catalyst is also an effective catalyst for the methanation reaction $(CO + 3H_2 = CH_4 + H_2O,\ MTN)$ in the temperature range of 250–400 °C [6]. Lee and co-workers [4] reported that a Ni metal catalyst pretreated by an oxidation and reduction process showed superior activity for CO removal via WGS and MTN reactions. Thus they stated that the MTN reaction, which consumes the hydrogen used as the fuel source of the fuel cell, must be suppressed to conserve the hydrogen energy.

In this study, an attempt is made to develop an effective MTS Ni metal catalyst that suppresses the MTN side-reaction. A comparative study is performed on a Ni metal catalyst and a modified Ni metal catalyst for the WGS reaction.

2. Experimental

2.1. Catalyst preparation

The Ni metal catalyst was prepared by pre-drying black and spherical Ni metal powder (Nano Technology, Inc.) in 70 vol.% H_2/He at 450 °C for 5 h. After the pretreatment process, the mean diameters of the nickel powders were (determined) by means of a particle-size analyzer (DT-1200, Micromeritics). The treated nickel powder catalyst has an average particle size of about 3.4 μm, i.e., higher than the 2.9 μm of bare nickel powder.

For the potassium-modified Ni metal catalyst, 5 wt.% potassium of support was impregnated over the Ni metal powder via the use

* Corresponding author. Tel.: +82 42 860 3504; fax: +82 42 860 3739.
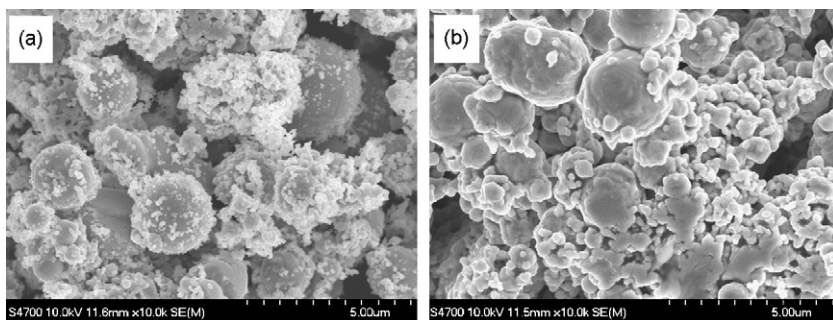*E-mail address:* deodor@kier.re.kr (J.-S. Park).

Fig. 1. FE-SEM images of (a) Ni metal powder and (b) potassium-impregnated Ni powder catalysts.

of an aqueous solution of $K(NO_3)$ (JUNSEI CHEMICAL Co. Ltd.), after which the catalyst was dried at 110 °C overnight and treated at 450 °C for 5 h in 70 vol.% H_2/He. Finally, the prepared powders were ground for 30 min.

The catalysts were characterized by Brunauer–Emmett–Teller (BET) surface area analysis (ASAP 2420), X-ray powder diffraction (XRD, D/MAX IIIC), field emission-scanning electron microscopy (FE-SEM, HITACHI S-7400), temperature-programmed desorption (CO_2-TPD, AutoChem II 2920), and diffuse reflectance infrared spectroscopy (DRIFTS, Nicolet 6700).

The DRIFTS experiment was conducted with a mercury cadmium telluride (MCT) detector. The sample was placed in a sample-cup and reduced in situ by 70 vol.% H_2/N_2 at 350 °C for 20 min. After purging with N_2 for 1 h, 250 ml min^{-1} of 1.0 vol.% CO/N_2 was introduced to the sample holder to determine the adsorption of CO at 350 °C, after which H_2 and steam were introduced with CO to examine the WGS and MTN reactions.

2.2. Water–gas shift (WGS) reaction test

The WGS reaction test was performed under more severe condition, namely, 60.0 vol.% CO, and 40 vol.% H_2, compared with the reformate gas, which was 7.0 vol.% CO, 8.5 vol.% CO_2, 22.0 vol.% H_2O, 37 vol.% H_2 and the remainder N_2, in order to confirm the higher selectivity of the prepared catalyst for WGS than for MTN. The molar ratio of steam to carbon was 3.0. The metal catalysts were pelletized, crushed into 40–60 mesh and inserted in a quartz tube (ID = 4 mm). Prior to the reaction test, the catalyst was reduced by 70 vol.% H_2/N_2 at 350 °C for 30 min. The produced gases were passed first through a cold trap to remove liquid water, and then through a soap bubble flow meter (SENSIDYNE, Gilibrator 2) to calculate their composition. Finally, a same amount of produced gases were fed to the inlet line of a gas chromatograph (GC6890, Agilent) for quantitative analysis. The feed and converted mixture of gases were analyzed by an on-line GC equipped with two thermal conductivity detectors (TCDs). The CO conversion and CH_4 selectivity were calculated from the following relations:

$$CO \ conversion \ (\%) = \frac{moles \ of \ CO \ consumed}{moles \ of \ CO \ fed} \times 100 \qquad (1)$$

$$CH_4 \ selectivity \ (\%) = \frac{moles \ of \ CH_4 \ produced}{moles \ of \ CO \ consumed} \times 100 \qquad (2)$$

3. Results and discussion

3.1. Characterization of metal catalysts

The BET surface areas of the Ni metal and modified Ni powders were 2.0 and 1.1 m^2 g^{-1}, respectively. As expected, the surface area of the modified Ni powder is diminished with surface impregnation. The FE-SEM images of the Ni metal powder and potassium-impregnated Ni powder catalysts are given in

Fig. 1(a) and (b), respectively. The nano-sized Ni particles in Fig. 1(a) are agglomerated after pre-drying and grinding, whereas the potassium-impregnated catalyst over Ni powder (Fig. 1(b)) has a smooth surface like a coated film.

The XRD patterns of the metal powder catalysts are given in Fig. 2. The peaks of the catalysts at 2θ = 44.5, 51.8 and 76.4 are identified as the typical diffraction peaks of Ni metal, while potassium over modified metal powder presents the state of the oxide, K_2O. From the XRD data, the interplanar spacing (d) of nickel was calculated by means of Bragg's law. For Ni, d_{111} and d_{220} are 2.0366 and 1.2467 Å, and for the potassium-modified Ni are 2.0364 and 1.2468 Å. This shows that there is no difference in the lattice parameter of nickel on impregnation with potassium.

The XRD results of Fig 2 and the BET surface area and FE-SEM studies indicate that the impregnated potassium is present only on the surface of the Ni powder. This means that if the potassium-modified Ni catalyst shows a higher selectivity for the WGS reaction than the MTN side-reaction, then the surface properties of potassium must play an important part in the selectivity of the WGS reaction because the Ni metal catalyst is active for the MTN reaction rather than for the WGS reaction in the CO-containing gas.

The TPD results for the metal powder catalysts are illustrated in Fig. 3. The TPD experiment was carried out to measure the basic properties of the catalyst with CO_2 as a probe molecule. As shown in Fig. 3, the potassium-modified Ni metal catalyst gives a maximum peak at ca. 82 °C with a shoulder at ca. 91 °C, and a broad peak around 360 °C with a small peak at ca. 260 °C. On the other hand, two broad and low-intensity peaks around 68 and 327 °C are observed for the Ni metal catalyst. Diez et al. [7] deconvoluted their CO_2-TPD data to quantify the density of the base
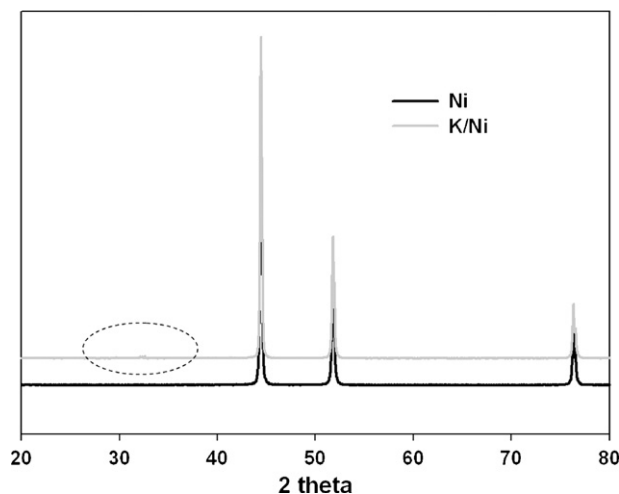

Fig. 2. XRD patterns of (a) Ni metal powder and (b) potassium-impregnated Ni powder catalysts (circle indicates potassium-related pattern).
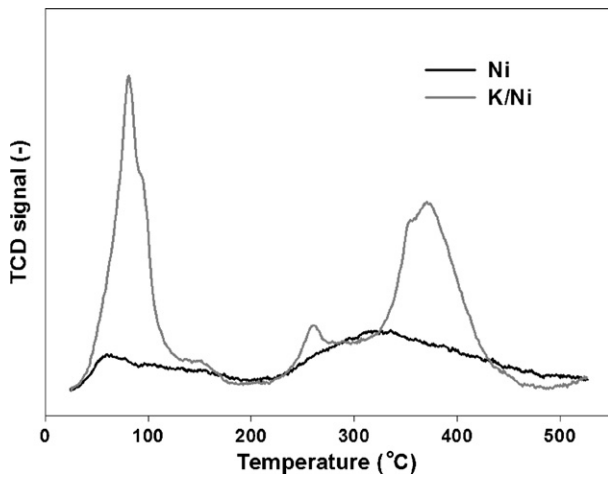
Fig. 3. TPD results for metal powder catalysts.

sites for MgO and the alkali-promoted MgO catalysts: the low-temperature peak at 87–107 °C was assigned to CO_2 absorbed on weakly basic OH groups, whereas the high-temperature peak above 170 °C was assigned to the release of carbonates from the medium and strong base sites. Considering that the present data are based on these deconvolution regions, differences are observed in the surface base properties between the Ni metal and the modified Ni metal catalysts. The base densities of the weak and strong sites for the modified Ni catalyst are significantly increased compared with those of the Ni metal catalyst, indicating that the base property, particularly weakly OH group, is introduced by the impregnation of alkali metal on the Ni metal catalyst.

The DRIFTS spectra are displayed in Figs. 4 and 5. The CO adsorptions over metal catalysts at 350 °C are shown in Figs. 4(a) and 5(a), the results of the reaction with H_2 and adsorbed CO over metal catalysts in Figs. 4(b) and 5(b), and the results of simultaneous reaction with H_2, steam and adsorbed CO over the metal catalysts in Figs. 4(c) and 5(c). As shown in Fig. 4(a), bands at 2173 and 2115 cm^{-1} are present for all catalysts and are attributed to the CO species adsorbed on the Ni sites [8,9]. On the other hand, the Ni and modified Ni catalysts differ when subjected to hydrogen or hydrogen and steam. As expected, the MTN reaction between CO and H_2 takes place over the Ni catalyst (Fig. 4(b) and (c)), and the peaks of the C–H bands of gaseous CH_4 appear at 3016 and 1304 cm^{-1}
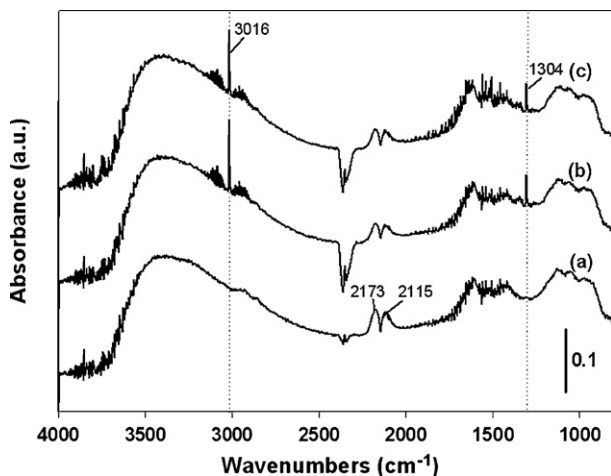

Fig. 4. DRIFTS spectra over the Ni metal catalyst at 350 °C. (a) Results of CO adsorption; (b) results of reaction with H_2 and adsorbed CO; (c) results of simultaneous reaction with H_2, steam and adsorbed CO over Ni metal catalyst.
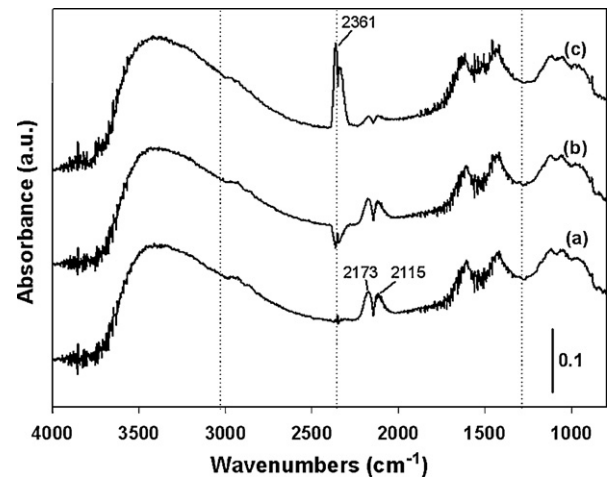

Fig. 5. DRIFTS spectra over potassium-impregnated Ni metal catalyst at 350 °C. (a) Results of CO adsorption; (b) results of reaction with H_2 and adsorbed CO; (c) results of simultaneous reaction with H_2, steam and adsorbed CO over potassium-impregnated Ni metal catalyst.
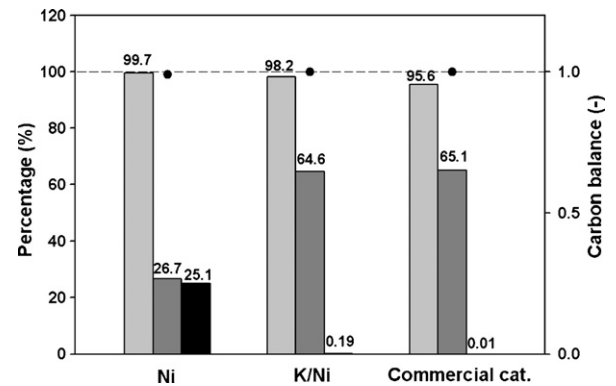

Fig. 6. Comparison of three different catalysts for WGS reaction at 350 °C and GHSV of 4000 h^{-1}. Gray bar: CO conversion (%); dark gray bar: H_2 production (%); black bar: CH_4 production (%); black dot: carbon balance (–).

[8,9]. By contrast, no C–H bands are observed over the K/Ni catalyst in Fig. 5(b) and (c). Instead, with the introduction of steam, the intensity of CO adsorbed over the metal catalyst was decreased and the gaseous CO_2 peak appeared at 2361 cm^{-1} (Fig. 5(c)). In other words, when the Ni metal powder is impregnated with potassium, the selectivity of the WGS reaction is higher than that of the
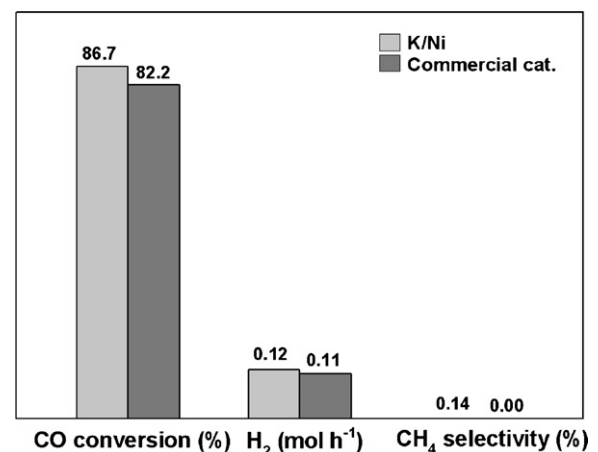

Fig. 7. Comparison of potassium-impregnated Ni and commercial catalysts for WGS reaction at 350 °C and GHSV of 80 000 h^{-1}.
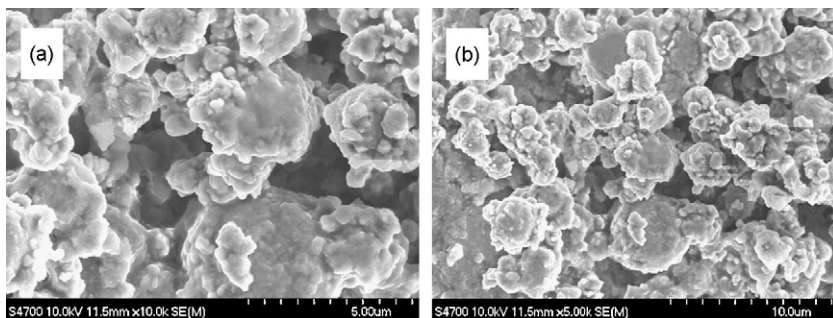
Fig. 8. FE-SEM images comparing (a) fresh and (b) used K/Ni metal catalyst.

MTN reaction. This may have been the cause of the large amount of weakly basic OH groups over the K/Ni catalyst, as discussed in the CO_2-TPD results. Generally, two main schemes have been proposed for the WGS reaction, namely, a redox mechanism [3] and a surface formate mechanism [10,11]. The latter involves reaction through an adsorbed surface intermediate, which is formed by the $CO_{ads} + OH_{ads}$ reaction, and is further decomposed rapidly toward CO_2 and H_2 in the presence of steam. If this surface formate mechanism is applicable to the Ni catalyst [12], a large amount of adsorbed hydroxyl groups are important to form the surface intermediate and the potassium is sufficient to supply active OH groups to the CO adsorbed on the Ni metal catalyst.

3.2. WGS reaction test

The CO conversion, the amounts of H_2 and CH_4 produced, and the carbon balance during the WGS reaction are presented in Fig. 6. The gas-hourly space velocity (GHSV) was $4000 \, h^{-1}$ and the commercial catalyst for the WGS reaction was used for comparison. The Ni metal and potassium-modified Ni metal catalysts exhibit a similar CO conversion of above 98%. Most of the adsorbed CO over the Ni catalyst is, however, converted to methane, with 25.1% of the methane being generated by the side-reaction, while less hydrogen was produced than over the K/Ni catalyst. Interestingly, the impregnation of potassium over the Ni metal powder suppresses the MTN side-reaction to 0.19% and CO is converted to CO_2 and H_2 with steam through the WGS reaction. The performance of the K/Ni catalyst is similar to that of the commercial WGS catalyst in terms of CO conversion, and H_2 and CH_4 production. The carbon balance is about 1.0 for all experiments.

The K/Ni and commercial WGS catalysts under a GHSV of $80\,000 \, h^{-1}$ are compared in Fig. 7. The K/Ni metal is a superior catalyst even at the relatively high GHSV.

A Ni-based catalyst usually suffers from coke formation [13]. In order to validate the non-coke formation, the FE-SEM image for a potassium-modified nickel catalyst after the water–gas shift reaction at $350\,°C$ for $20\,h$ under the severe condition of GHSV = $80\,000 \, h^{-1}$, SV = $80\,000 \, h^{-1}$ is present in Fig. 8. The nickel catalyst does not suffer from further morphological changes compared with the fresh catalyst and there is no accumulation of carbon under the chosen conditions.

4. Conclusions

A comparative study has been performed to investigate the effectiveness of a Ni metal catalyst before and after impregna-

tion with potassium for the water–gas shift (WGS) reaction. The potassium-modified Ni metal is both more active and more selective for the WGS reaction than the unmodified Ni catalyst, which has found limited application for the WGS reaction due to its catalysis of the undesirable methanation reaction (MTN). Furthermore, there is no carbon deposition over the modified Ni catalyst. The amount of H_2 produced and the CO conversion via WGS over the potassium-modified Ni catalyst are higher than those of commercial high-temperature shift (HTS) catalysts under severe experimental conditions (GHSV = $80\,000 \, h^{-1}$, CO 60% and H_2 40%). The suppression of MTN over the modified Ni metal is attributed to the action of the incorporated potassium in increasing the density of the active hydroxyl group that takes part in the WGS reaction to form the intermediate. Most importantly, the modified Ni metal catalyst has the potential to reduce the volume of the WGS reactor in applications of micro-channel reactors or filter reactors of the thin-disc type for the single-step WGS reaction. The modified Ni metal catalyst can also act as a membrane support and a WGS catalyst for the simultaneous reaction and separation process required in hydrogen production, because Ni metal with a thin-disc shape is used as a support for the hydrogen membrane.

References

[1] T.A. Semelsberger, R.L. Borup, Int. J. Hydrogen Energy 30 (2005) 425–435.
[2] K.R. Hwang, S.H. Cho, S.K. Ihm, C.B. Lee, J.S. Park, J. Chem. Eng. Jpn. 42 (2009) 1–5.
[3] Y. Li, Q. Fu, M.F. Stephanopoulos, Appl. Catal. B 27 (2000) 179–191.
[4] S.H. Kim, S.W. Nam, H.I. Lee, Appl. Catal. B: Environ. 81 (2008) 97–104.
[5] K.R. Hwang, S.K. Ihm, J.S. Park, Korean J. Chem. Eng. 27 (2010) 816–821.
[6] S. Takenak, T. Shimizu, K. Otsuka, Int. J. Hydrogen Energy 29 (2004) 1065–1073.
[7] V.K. Diez, C.R. Apesteguia, J.I. Di Cosimo, J. Catal. 240 (2006) 235–244.
[8] O. Demoulin, M. Navez, P. Ruiz, Catal. Today 112 (2006) 153–156.
[9] G. Jianzhong, H. Zhaoyin, G. Jing, Z. Xiaoming, Chin. J. Catal. 28 (2007) 22–26.
[10] T. Shido, Y. Iwasawa, J. Catal. 141 (1993) 71–81.
[11] G. Jacobs, P.M. Patterson, U.M. Graham, D.E. Sparks, B.H. Davis, Appl. Catal. 269 (2004) 63–73.
[12] M.S. Spencer, Catal. Today 12 (1992) 453–464.
[13] L. Barelli, G. Bidini, F. Gallorini, S. Servili, Energy 33 (2008) 554–570.